

Comparative Study of Differential Scanning Calorimetry (DSC) Analysis and Rheology of HDPE-Typha and PLA-Typha Biocomposites and Photo-Aging of HDPE-Typha Biocomposites

Babacar Niang^{1,*}, Abdou Karim Farota¹, Abdoul Karim Mbodji¹, Nicola Schiavone², Haroutioun Askanian², Vincent Verney², Abdoulaye Bouya Diop¹, Diène Ndiaye¹, Bouya Diop¹

¹Laboratory of Atmospheric and Ocean-Material Sciences, Energy, Device, Training and Research Unit of Applied Sciences and Technologies, Gaston Berger University, Saint-Louis, Senegal

²Clermont Ferrand Institute of Chemistry, Clermont Auvergne University, National Centre for Scientific Research, SIGMA Clermont, Clermont-Ferrand, France

Abstract This work focuses on the comparative study of the thermal, viscoelastic and photochemical durability of biocomposites made from two matrices (PLA and HDPE) and Typha stem powder by the extrusion process. Differential scanning calorimetry analysis shows that the biocomposites have higher crystallinity values than the virgin matrices, and it is demonstrated that the variation in molecular weight or crystallinity causes a shift in compaction and a slight shift in melting temperature to higher values than the virgin matrices. The rheological tests show an increase in storage and loss moduli reflecting a more elastic behaviour at higher Typha powder weights. shear thinning behaviour was observed for all samples. The viscoelastic properties of HDPE biocomposites are superior to those of PLA. The study of photodegradation revealed the existence of chain cutting and recrosslinking phenomena in our samples. The mechanisms involved in photooxidation occurred jointly within the biomaterials.

Keywords Rheology, Thermal analysis, Photo-aging, Biocomposites

1. Introduction

Technology has contributed to major development of humanity, but often at the expense of the environment and natural resources. Toxic and non-degradable materials have for many years been the basis on which this development has been achieved. The growing awareness of sustainability issues has led governments and companies to move towards the use of environmentally appropriate materials. The principles of reduction, reuse and recycling are increasingly being applied in practice, whether in materials, processing or product design and development. The re-integration of recycled materials into the product life cycle allows for a visible reduction in the use of virgin raw materials, thus reducing the impact on natural resources [1], [2]. Against this background of major environmental change. Wood plastic composites (WPC) are mixtures of wood flour (WF) and thermoplastic resins, such as polypropylene (PP),

polyethylene (PE) or polyvinyl chloride (PVC). WPCs can be made from environmentally friendly materials, such as wood waste, unused natural resources and recycled thermoplastic resins [3,4]. WPCs have many excellent properties, such as high durability, specific strength, specific stiffness and wear resistance. They also have high moulding performance and a texture similar to that of solid wood. The main application of WPCs is in the manufacture of outdoor decking. However, as WPC technology continues to mature and manufacturing processes improve, WPCs can also be used in other industries, such as automotive and consumer electronics [5,6].

Many types of naturally occurring fibres are mainly used in the production of biocomposites. Flax, hemp, jute, coir, cotton, sisal, kenaf, silk and bamboo are the most explored cellulosic fibres [7].

Migneault et al [8] studied the effects of wood fibre origin, proportion and chemical composition on the properties of wood-plastic composites (WPCs). Interestingly, WPCs based on pulp and paper sludge showed better overall properties compared to other raw materials. Csikós et al [9] produced a wood fibre composite based on poly(lactic acid) (PLA) and Filtracel EFC 1000 (Rettenmaier and Söhne

* Corresponding author:

niang.babacar1@ugb.edu.sn (Babacar Niang)

Received: Jan. 3, 2022; Accepted: Jan. 21, 2022; Published: Mar. 15, 2022

Published online at <http://journal.sapub.org/cmaterials>

GmbH) and investigated the surface of the wood fibres on the interfacial bonding between the wood fibres and the polymer matrix, as well as studies on spruce sawdust based composites, which showed that this fibre could be a potential filler for high density polyethylene (HDPE) based composites. Typha fibres are part of this wide range of fibres and are very abundant in South Saharan Africa. Many researchers have investigated the potential of Typha fibres as natural cellulosic reinforcing fibres in composites.

Different factors such as fibre loading, fibre surface modification, fibre chemical composition and process parameters can affect the characteristics and performance [11] [12] [13]. Depending on the final application of the composite, the polymer matrix is selected. Typha fibre has been tested in various matrices including polyester, polystyrene, low density polyethylene (LDPE).

In the present work, bio-composite fibres were developed from Typha fibre (TT) and polymeric matrices (PLA) and (HDPE) by an extrusion process. A comparative study of thermal properties by analysis (DSC) and rheology will be carried out, and the influence of photoveiling on the properties of the biocomposites will be followed to understand the influence and impacts of photodegradation mechanisms on the rheological properties of our samples.

2. Experimental

2.1. Materials

Poly(lactic acid) (PLA) is a thermoplastic polyester produced by fermentation of renewable agricultural raw materials followed by polymerisation. In this study, PLLA (PLA4032D) was used, which contained ~2% by weight D-lactic acid and had an average molecular weight of 190,000. It was purchased from Nature Works LLC. The density, melting point (T_m) and glass transition temperature of PLA4032D were 1.24 g/cm^3 , 170°C and 59.2°C respectively. The natural filler used was Typha stem powder. It was collected from the banks of the Senegal River, at Bango in the Saint Louis region. The plant was cut and air-dried and then undergoes mechanical grinding to transform the stems into powders. The shape of the powder varies from particles of approximately spherical geometry smaller than 50 microns to filaments larger than 1mm.

The HDPE was supplied in granular form by Nova Chemicals. Its melt index was 7.0 g/10 min at 190°C and its density at room temperature was 0.962 g/cm^3 .

2.2. Compounding and Processing

The Typha stem powder was oven dried at 105°C and the polymers (HDPE and PLA) at 60°C for 24 hours to remove moisture. The composites were developed in a HAAKE

Minilab twin screw extruder (Thermo Scientific), operating at a screw speed of 100 rpm, at a temperature of 180°C for 5 min. Four formulations of the composites were prepared with different filler contents equal to 0%, 25%, 35%, 45% by mass of Typha Rod (TT). The composites were then compression moulded using a Carver laboratory press at 180°C and 200 bar for 1 minute to obtain a film of approximately $150 \mu\text{m}$. This film is used for mechanical testing.

3. Rheological Characterization

The rheological characterization of the composites functions was carried out using dynamic low amplitude oscillatory shear tests. This method makes it possible to measure the dynamic properties of composites such as dynamic moduli G' , G'' , and the loss, complex and storage viscosity respectively η' , η'' , and η^* . The dynamic elastic moduli G' and η'' , help measure the elastic energy stored in the deformed material. This energy is reversible; it helps the material partially re-cover its shape before the deformation. While the dynamic moduli G'' and η' represent the dynamic loss modulus, they correspond to the amount of energy dissipated by the materials due to the interaction between the molecular chains of the polymers in shear. The variation of these moduli, according to the frequency and at a temperature equal to 180°C for biocomposites with different wood contents, is studied.

3.1. Differential Scanning Calorimetry Analysis

Thermal analysis of the biocomposite samples was carried out on a differential scanning calorimeter (METTLER TOLEDO DSC 3). All DSC measurements were performed with powdered samples of about $10 \pm 0.2 \text{ mg}$ under a nitrogen atmosphere with a flow rate of 20 ml/min . All samples were subjected to the same thermal experiment with the following thermal protocol:

- 1) First, the samples were heated from 25°C to 210°C at a heating rate of 10°C/min to eliminate any thermal history effect;
- 2) Second, the samples were cooled from 210°C to 40°C at a cooling rate of 10°C/min to detect the crystallization temperature (T_c);
- 3) Finally, the samples were heated from 25°C to 210°C at a heating rate of 10°C/min to determine T_m . T_m and the heat of fusion (ΔH_m) were obtained from the thermograms during the second heating. The values of ΔH_m were used to estimate the crystallinity degree (X_c). The degree of crystallinity (X_c) of the PLA and HDPE component was determined from the following equation [14] [15]

Table 1. Biocomposite size

Norme	Type d'éprouvette	l_3	l_1	b_2	b_1	h	L_0	L	Forme
ASTMD638	II	>183	$57 \pm 0,5$	$19 \pm 6,4$	$6 \pm 0,5$	$3,2 \pm 0,4$	$50 \pm 0,25$	135 ± 5	Haltère

$$X_c = \frac{\Delta H_m - \Delta H_c}{\Delta H_0 \times (1 - wTT)} \times 100$$

3.2. Study of Accelerated Photoaging of Biocomposites

The photoaging (figure 1) was carried out at 60°C in SEPAP 12/24 type chambers (Service d'Etude du Photo vieillissement Accéléré des Polymères) [16]. The irradiation chamber of this device has four 400 W medium pressure mercury vapour lamps whose borosilicate glass envelope filters wavelengths below 295 nm.



Figure 1. SEPAP 12/24 photoaging devices



Figure 2. SEPAP 12/24, Life cycle assessment tool for plastics and composites

The samples are fixed on a rotating turret (4 rpm) located in the centre of these four lamps. The temperature of the samples is monitored by a platinum probe in contact with a composite film attached to the turret (Figure 2). The humidity level in the chamber does not exceed 3%. Some irradiations were performed behind filters labelled F290 nm, F330 nm and F400 nm in order to study the impact of the irradiation wavelengths.

4. Results and Discussion

4.1. Study of the Characteristics of HDPE and PLA Matrix Composites

4.1.1. Rheology Results

The rheological properties of the samples in the molten state were determined by dynamic mechanical measurements. The storage modulus G' , loss modulus G'' and dynamic viscosity η^* were measured as a function of swept frequencies between 0.1 and 100 rad/s.

Figures 3 and 4 and 5 show the viscoelastic behaviour of HDPE/Typha materials through the dynamic moduli (G') and (G'') and the complex viscosity.

The dynamic storage (G') and loss moduli (G'') tend to increase with the proportion of typha powder (Figure 3 and 4). This results in a more elastic behaviour for high wood masses. Obviously, the complex viscosity of the pure polymer increases progressively with the increase of the powder content from 25% to 45% (Figure 5). This is because in filled systems, wood particles disrupt the flow of the pure polymer and impede the mobility of the chain segments in the direction of flow. These particles often occur in the form of aggregates.

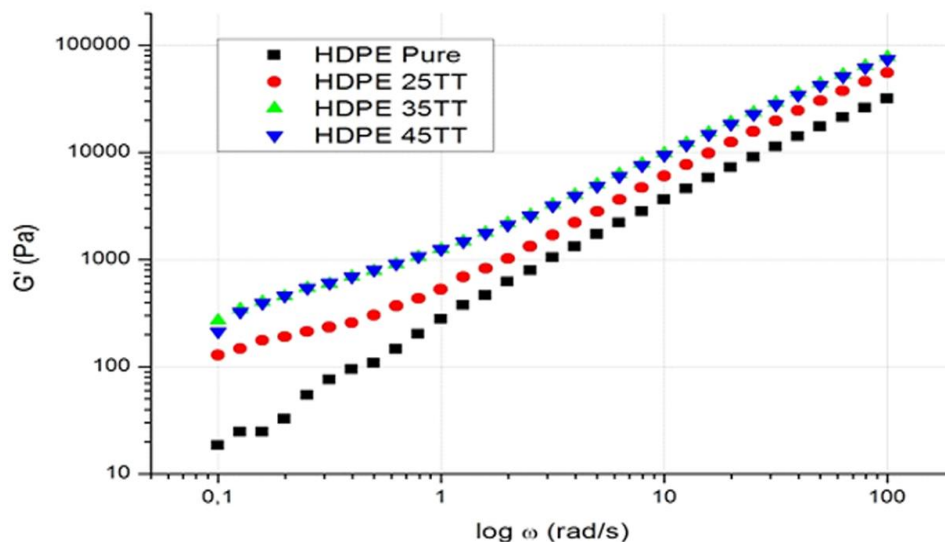


Figure 3. The variation of dynamic moduli (G') as a function of frequency with different percentages of typha stem

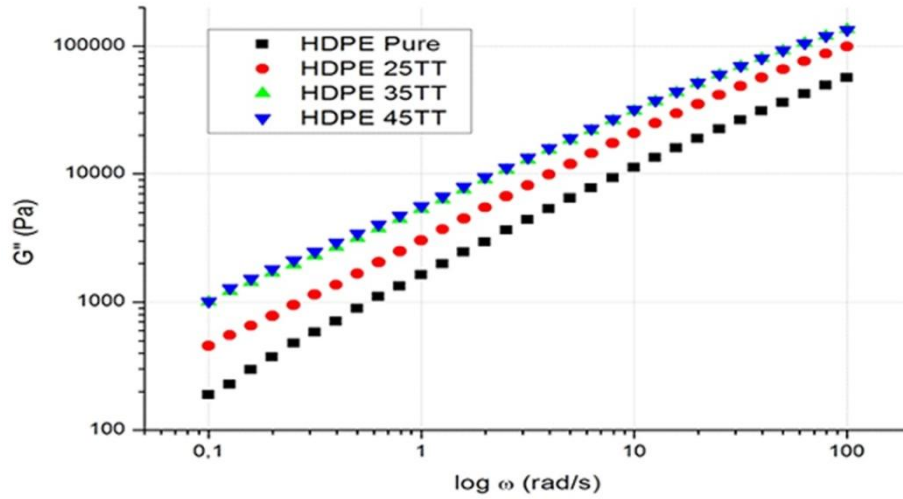


Figure 4. Variation of complex viscosity as a function of frequency of pure HDPE and its composites at $T = 180^{\circ}\text{C}$

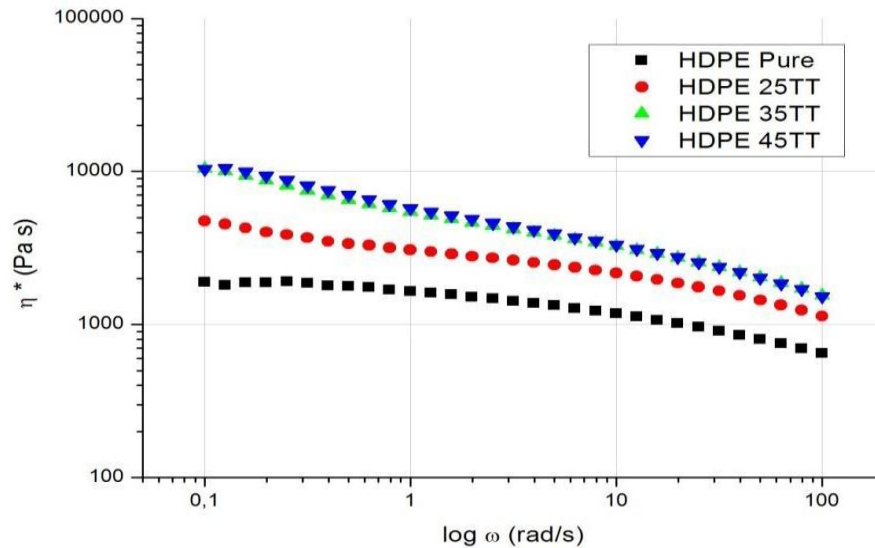


Figure 5. The Variation of the complex viscosity as a function of frequency of pure HDPE and its composites at $T = 180^{\circ}\text{C}$

This is also due to the inhomogeneous dispersion and alignment of the cellulose phase in the composites. These observations are confirmed by those of other authors [17], [18] [19]. Moreover, the moduli G' and G'' tend to have the same values above 35% (Figure 5). We observed a rheofluidic behaviour by shearing of the melt. The viscosity of the composites is strongly influenced by the shear rate. The composites show approximately the same viscosity above 35%. This is probably due to the alignment of the fibres at high shear rates. This reduces collisions between particles [17] [20]. In effect, the fluidity of the mixture is increased by increasing the oscillation frequency, which decreases the complex viscosity. This reduction in viscosity shows the pseudoplastic nature of the materials in the molten state.

In the low frequency range, the viscosity increases significantly with increasing fibre content of the composite material (Figure 5). The addition of fibres affects the stiffness, density and viscoelastic behaviour of a polymer [21], [22], [23].

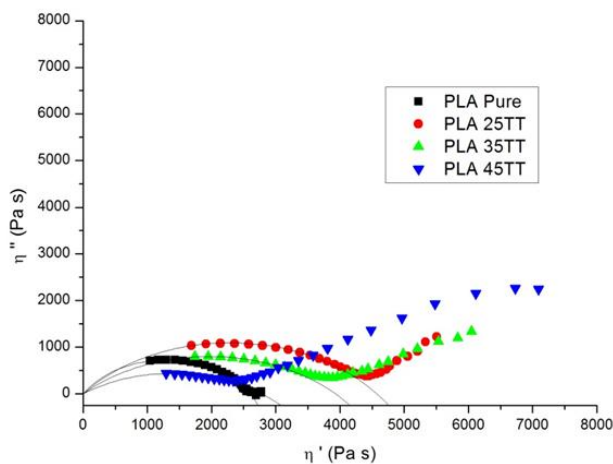
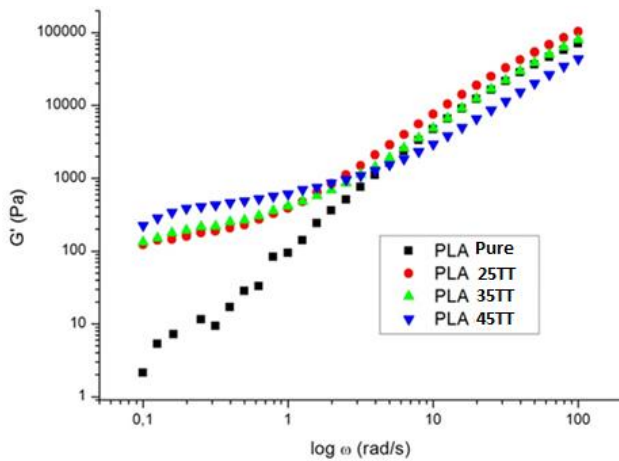
The highest values of complex viscosity were observed with the composite containing 45% by weight of typha fibres (Figure 5). In addition, the presence of agglomerates (due to their high fibre content) causes a flow resistance and an increase in the viscosity of the composites. This behaviour can be explained by a higher interaction rate between the polymer matrix and the content. This forces the mixture to have a higher shear stress and longer relaxation times to the flow of the composites [24]. The rheological properties of high density polyethylene show the same shear rheofluidising behaviour. The moduli of elasticity show an improvement in the dynamic behaviour of the composites.

While under the same conditions, we have presented in figure 6 the variations in viscosity in the complex plane of pure PLA and the composites. It allows an extrapolation of the arc constructed on the complex graph to determine the Newtonian viscosity. Table 2 shows the values of the Newtonian viscosity determined for the PLA-TT samples analysed:

Table 2. Newtonian viscosity values of the samples

Echantillons	η (Pa s)
PLA Pur	2606
PLA 25TT	4576
PLA 35TT	3929
PLA 45TT	2780

The results show a 76% increase in viscosity when 25% of the PLA is replaced by fibre (PLA/25TT); this viscosity decreases when the amount of filler is increased. He also found that the viscosity of the material with 45% fibre (PLA/45TT) almost matches that of PLA with a 6% higher value. However, an increase in the amount of filler should result in a reduction in viscosity.

**Figure 6.** Complex plane diagrams for all composites at $T = 180^\circ\text{C}$ **Figure 7.** Variations in storage modulus G' as a function of frequency for pure PLA and its composites at $T = 180^\circ\text{C}$

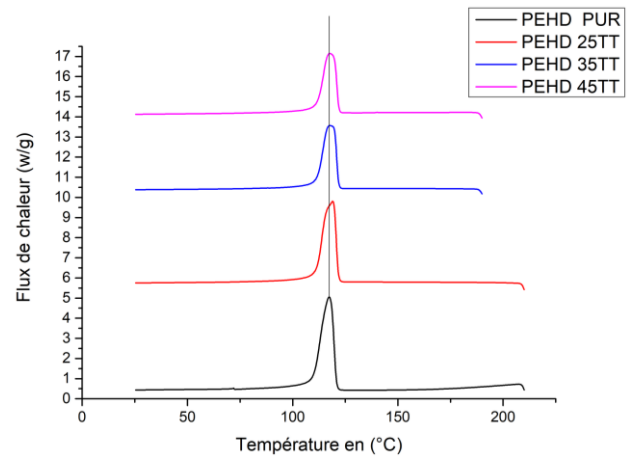
The change in viscosity is often caused by the disruption of normal polymer flow; filler particles prevent chain mobility as previously observed in HDPE-based composites. All composite samples show a deviation from the circular behaviour favouring the shift of the Newtonian plateau at low frequencies (Figure 6). This phenomenon is characteristic of gel behaviour, indicating that at different powder concentrations, the level of interaction between the

matrix and the filler is not the same at different applied frequencies [25] [26]. In fact, at low frequencies, the viscosity increases strongly with the typha powder content, as shown by the variations in the storage modulus (G') of the composites (Figure 7). In general, all biocomposites (HDPE-Typha and PLA-Typha) exhibit rheofluidic behaviour by shearing of the melt is observed. The viscosity of the composites is strongly influenced by the shear rate [27].

The storage moduli of the samples of the different biocomposites indicate that the stress transfers from the matrix to the filler are more important especially for the higher powder content. Referring to the data of storage modulus (G'), serving as a measure of molecular stiffness, it can be concluded that with the addition of TT as reinforcement the biomaterials become stiffer [28] [29].

4.1.2. Thermal Analysis by Differential Scanning Calorimetry

Differential scanning calorimetry (DSC) measurements were performed on the different typha stem composite samples. The parameters resulting from the measurements are the melting temperature (T_f), the crystallisation temperature (T_c), the enthalpy of crystallisation (ΔH_c), the enthalpy of fusion (ΔH_m) and the percentage of crystallinity (% X_c). Figure 8 and Figure 9 show the DSC thermograms of the cooling and heating curves of HDPE and its composites respectively. Table 2 summarises the thermal properties of the composites. The thermograms show endothermic peaks between 133°C and 135°C during heating and exothermic peaks between 118°C and 120°C during cooling (Table 2).

**Figure 8.** DSC cooling thermograms of pure HDPE and its composites containing different percentages of typha stem

The combination of wood fibres with the matrix tends to increase the melting temperature of the composite materials. Furthermore, it is also noted that the melting temperature increases with an increase in the reinforcement ratio. This can be explained by the fact that the Typha fibres intercalated in the polymer matrix act as insulators and slow down the heat conduction process [30].

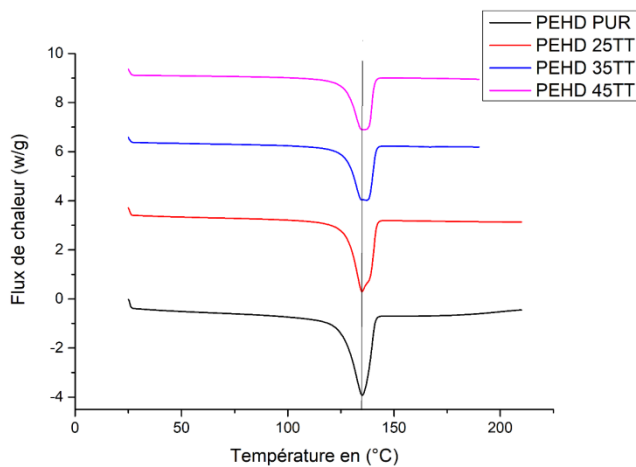


Figure 9. Thermograms of DSC heatings of pure HDPE and its composites containing different concentrations of typha stem

Table 3. Thermal properties of pure HDPE and its composites

Echantillons	T _c (°C)	T _m (°C)	ΔH _m (J/g)	ΔH _c (J/g)	X _c (%)
PEHD Pur	119,27	133,69	179,15	181,74	61,10
PEHD 25	120,45	133,00	156,73	163,94	71,30
PEHD 35	118,98	136,53	119,67	128,00	62,80
PEHD 45	119,18	135,73	107,07	119,75	66,50

On the one hand, the results obtained from the calorimetric analysis show an increase in the degree of crystallinity with the addition of typha fibres (Table 3). The fibres could represent nucleation centres. The increase in crystallinity may also be due to changes in molecular weight that occur during polymer degradation. This leads to chain breakage and oxidation reactions on the surface. All these processes increase the free energy of the biocomposite crystals and catalyse it to early crystallisation and probably secondary crystallisation. The latter is described as a slow process that occurs in interspherulitic regions [31] and/or within spherulites [32]. These results are in agreement with other literature studies and show that the creation of short chains during polymer degradation leads to chemicrystallisation [33]. In the composite, the increase in crystallinity is due to a decrease in molecular weight [30]. The most important effect of wood fibre on the semi-crystalline structure of HDPE is its ability to act as a nucleating agent, which promotes the crystallisation of HDPE. It should be remembered that there are two types of nucleation. The formation of a bubble within a perfectly uniform liquid is called homogeneous nucleation. The presence of a second phase, or simply a depression in the surface tension of the polymer, necessarily leads to heterogeneous nucleation. Nucleation is defined as a dispersion of fine solid particles distributed in the matrix. The variation in molecular weight or crystallinity causes a shift in compaction and a slight shift in melting temperature to values higher than that of pure HDPE. Indeed, this process is sometimes attributed to the formation of secondary lamellar stacks consisting of thinner crystals that are inserted between primary lamellar stacks consisting of the thicker crystals. On the other hand, secondary crystallisation is

attributed to the insertion of lamellae of regular sizes between the primary lamellae.

On the other hand, the measurements carried out on the biocomposites by DSC analysis made it possible to determine the thermal parameters such as the melting (T_f), glass transition (T_g) and crystallisation (T_c) temperatures, the enthalpies of crystallisation (ΔH_c (J/g) and melting (ΔH_f (J/g)) and the percentage of crystallinity (c). Figure 10 shows the DSC thermograms of PLA and these composites at different reinforcement rates (Typha).

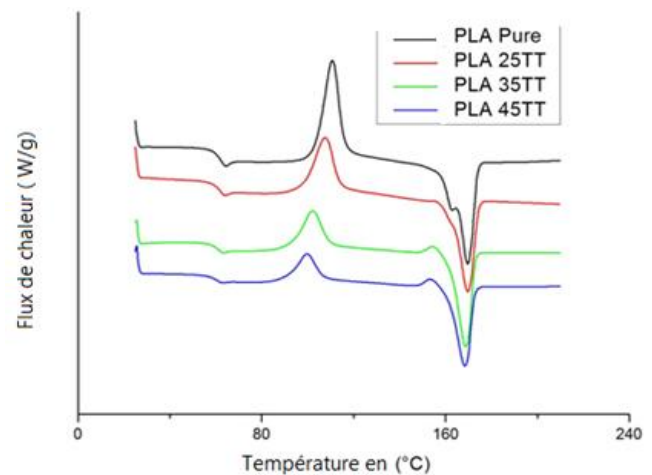


Figure 10. Melting thermograms of pure PLA and its composites

The glass transition temperature (T_g) does not show any variation and the T_f temperature is very slightly reduced in the presence of the powder. However, the phenomenon of the double melting peak is reduced after the addition of the powder. usually the polyesters show a double melting peak and the presence of crystals of different sizes. The presence of a single peak in biocomposites can be explained by the reduced mobility of non-entangled chains, compared to pure PLA. Moreover, this explanation is also compatible with the reduction of the cold crystallisation temperature and the increase in the degree of crystallinity (Table 3). This highlights an increase in the order of PLA chains [134]. Furthermore, typha fibres act as nucleating agents and therefore the crystallisation of PLA takes place differently depending on the presence or absence of fibres [34] [35]. The presence of fibres decreases T_f compared to pure PLA, resulting in smaller crystals or crystals with more defects. The crystallinity of PLA increases in the presence of fibres, from 4% for pure PLA to values between 12 and 30% for biocomposites (Table 4). The presence of fibres therefore leads to the creation of more crystals (X_c(%) increases). It would seem that the smaller the diameter of the fibres, the higher the crystallinity rate. In this constructive and comparative analysis, the evolution of the microstructure during deformation at imposed temperature showed that the biocomposites (HDPE/TT) with the highest degree of crystallinity had better thermomechanical and viscoelastic properties. We believe that there is a deformation of the overall semi-crystalline structure (amorphous and crystalline phase) of the biocomposites. The crystalline and amorphous

zones of the semi-crystalline polymers (PLA and HDPE) subjected to mechanical loading undergo shear deformations according to the orientation of the crystalline lamellae in the spherulites. At the first values of the deformation, the phenomenon of interlamellar separation and slippage takes place, followed by the shearing mechanism of the stacking of crystalline lamellae and amorphous phase. The long period then increases in value as the biocomposite deforms, this mechanism being higher for HDPE-based biocomposites. The shear is then transmitted to the crystallites inducing the sliding of the macromolecular chains of the crystalline lamellae in relation to each other and they tend to orient themselves according to the direction of the stress. At high deformation, we could observe a fragmentation of the crystalline structure. However, at an imposed deformation and temperature, under the effect of the stress, we can observe the phenomenon of rheofluidification by shearing of all the samples.

Table 4. Thermal properties of pure PLA and its composites

Echantillons	T_g (°C)	T_c (°C)	T_f (°C)	ΔH_c (J/g)	ΔH_f (J/g)	X_c (%)
PLA Pure	61	111	170	27	31	4%
PLA 25TT	61	108	170	18	27	12%
PLA 35TT	61	102	169	13	26	22%
PLA 45TT	61	100	168	8	23	30%

After presenting the constructive and compractive analysis of the properties of the two biocomposites (HDPE/TT) and (PLA/TT). In the following, we present the analysis and interpretation of the mechanisms involved in the photo-aging of the biocomposites.

4.1.3. Influence of Accelerated Photoaging on Rheological Properties

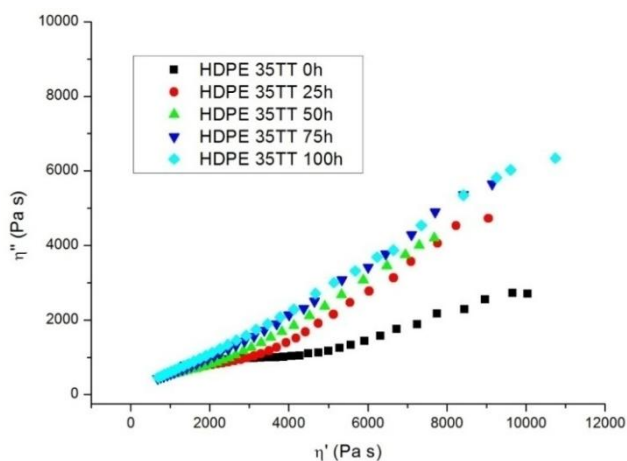


Figure 11. Cole-Cole diagram for biocomposite films (HDPE 35TT) irradiated in SEPAP 12-24

The monitoring of different materials by rheological measurements during ageing helps to understand the mechanisms of photodegradation. Indeed, dynamic rheology is a tool that allows the detection of minimal changes at the

molecular level. Thus, possible cuts or recombinations of chains taking place during photochemical degradation will be easily detected [36], [37]. A frequency scan is performed between each ageing period at 180°C for pure HDPE and its composites. The accelerated photoaging results are shown in the complex plane for the biomaterials respectively in Figure 11.

The Cole Cole diagram shows the evolution of these two zones over the irradiation times. The first zone in the form of an arc in Figure 11 decreases rapidly until it is no longer observable, which means that chain breaks occur during photoaging [38]. The second zone corresponds to the straight line whose slope increases up to 75 hours of irradiation then decreases for the last exposure time at 100 hours. It is in this second zone that the formation of a cross-linking network due to recombination of the chains takes place [38].

These behaviours observed during photodegradation reflect chain breaks in the first stage and the formation of a cross-linking network due to chain recombination in the second stage. It is interesting to observe that both mechanisms (chain splitting and recombination) of photooxidation occur together in the material. Chain splitting predominates for a population that can then be assimilated to the HDPE chains in the biocomposite. The cross-linkages of this population are predominant up to 75h of irradiation, and then become a minority compared to the macromolecular chain splits [39], [40]. Under irradiation, the lignin component of the plant fibre considered as well as the key structures involved in its degradation generate phenoxy radicals, and the phenols are also oxidised. The influence of the presence of fibres in composites is expressed in the durability of the biocomposite by the modification of the kinetics of photooxidation. Indeed, the presence of fibres leads to an increase in the oxidation rate of the polymer matrix after the induction period. This effect is increasingly accentuated as the amount of fibre in the composite increases. This can be explained by the radical species produced by photooxidation [41]. Thus, the fibre acts as an initiator and/or accelerator of photooxidation [42].

5. Conclusions

Biocomposite samples containing Typha fibres were obtained and successfully analysed. Based on the results of differential scanning calorimetry, rheology and photo-wetting, it was found that Typha fibres can be added to biosourced matrices to obtain good properties.

The results obtained from the calorimetric analysis show an increase in the degree of crystallinity with the addition of typha fibres. The fibres could represent nucleation centres. The increase in crystallinity may also be due to changes in molecular weight that occur during polymer degradation. This leads to chain breakage and oxidation reactions on the surface. All these processes increase the free energy of the biocomposite crystals and catalyse it to early and probably secondary crystallisation. The most important effect of wood

fibre on the semi-crystalline structure of HDPE and PLA is its ability to act as a nucleating agent which promotes crystallisation. The presence of fibres decreases Tf compared to pure PLA and HDPE, resulting in smaller or more defected crystals. The crystallinity of biocomposites increases in the presence of fibres. For the same concentration of reinforcement, HDPE-Typha biocomposites have the highest degree of crystallinity. The dynamic storage (G') and loss (G'') moduli tend to increase with the proportion of typha powder. The complex viscosity of the pure polymer increases progressively with increasing powder content from 25% to 45% for all biocomposites, but the HDPE matrix biocomposites show higher viscosity values than the PLA matrix biocomposites. We observed a rheofluidic behaviour by shearing of the melt. The viscosity of the composites is strongly influenced by the shear rate. The results of the photo-evaporation of the biocomposite samples (HDPE-Typha) show the existence of two behaviours, observed during the photodegradation, reflecting chain cleavages in a first step and the formation of a cross-linking network due to chain recombination in a second step. It is interesting to observe that both mechanisms (chain splitting and recombination) of photooxidation occur together in the material. Chain splitting predominates for a population that can then be assimilated to the HDPE chains in the biocomposite. The cross-links of this population are predominant up to 75h of irradiation, and then become a minority compared to the macromolecular chain splits.

REFERENCES

- [1] L. A. Dobrzanski, "Significance of materials science for the future development of societies," *J. Mater. Process. Technol.*, vol. 175, no. 1–3, pp. 133–148, 2006.
- [2] A. N. Klein, M. C. Fredel, and P. A. P. Wendhausen, "NOVOS MATERIAIS: Realidade e tendências de desenvolvimento," *desenvolvimento.gov.br*, 2015. MORENO, Diego David Pinzón et SARON, Clodoaldo. Low-density polyethylene waste/recycled wood composites. Composite Structures, 2017, vol. 176, p. 1152-1157.
- [3] KIM, Jin Kuk et PAL, Kaushik. Recent advances in the processing of wood-plastic composites. 2010.
- [4] GARDNER, Douglas J., HAN, Yousoo, et WANG, Lu. Wood-plastic composite technology. Current Forestry Reports, 2015, vol. 1, no 3, p. 139-150.
- [5] Väisänen, T.; Das, O.; Tomppo, L. A review on new bio-based constituents for natural fiber-polymer composites. *J. Clean. Prod.* 2017, 149, 582–596.
- [6] Ramamoorthy, S.K.; Skrifvars, M.; Persson, A. A review of natural fibers used in biocomposites: Plant, animal and regenerated cellulose fibers. *Polym. Rev.* 2015, 55, 107–162.
- [7] Gurunathan, T.; Mohanty, S.; Nayak, S.K. A review of the recent developments in biocomposites based on natural fibres and their application perspectives. *Compos. Part A: Appl. Sci. Manuf.* 2015, 77, 1–25.
- [8] Migneault, S.; Koubaa, A.; Perré, P. Effect of fiber origin, proportion, and chemical composition on the mechanical and physical properties of wood-plastic composites. *J. Wood Chem. Technol.* 2014, 34, 241–261.
- [9] Csikós, Á.; Faludi, G.; Domján, A.; Renner, K.; Móczó, J.; Pukánszky, B. Modification of interfacial adhesion with a functionalized polymer in PLA/wood composites. *Eur. Polym. J.* 2015, 68, 592–600.
- [10] Tazi, M.; Sukiman, M.S.; Erchiqui, F.; Imad, A.; Kanit, T. Effect of wood fillers on the viscoelastic and thermophysical properties of HDPE-wood composite. *Int. J. Polym. Sci.* 2016, 2016, 9032525.
- [11] Ramanaiah, K., A. Ratna Prasad, and K. H. Chandra Reddy. 2011. Mechanical properties and thermal conductivity of Typha angustifolia natural fiber-reinforced polyester composites. *International Journal of Polymer Analysis and Characterization* 16 (7): 496–503. doi:10.1080/1023666X.2011.598528.
- [12] Rezig, S., F. Khoffi, Y. Ben Mlik, M. Jaouadi, S. Msahli, and B. Durand. 2015. Flexural properties of typha natural fiber-reinforced polyester composites. *Fibers and Polymers* 16 (11): 2451–57. doi:10.1007/s12221-015-5306-x.
- [13] Ramesh, M., C. Deepa, M. Tamil Selvan, and K. H. Reddy. 2020. Effect of alkalization on characterization of ripe bulrush (Typha Domingensis) grass fiber reinforced epoxy composites. *Journal of Natural Fibers* 1–12.
- [14] Dorlot, J.M., Bailon, J.P. and Masounave, J. (1986) Des matériaux. 24-44 éditions, Polytechnique de Montréal, Montréal.
- [15] Ndiaye, D., Diop, B., Thiandoume, C., Fall, P.A., Farota, A.K. and Tidjani, A. (2012) Morphology and thermo mechanical properties of wood/polypropylene composites. *Polypropylene*, 4, 730-738.
- [16] H. B. Zouari et al., « Influence of in situ photo-induced silver nanoparticles on the ageing of acrylate materials », *Journal of Photochemistry and Photobiology A: Chemistry*, vol. 408, p. 113112, mars 2021, doi:10.1016/j.jphotochem.2020.113112.
- [17] H.-S. Kim, H.-S. Yang, H.-J. Kim, et H.-J. Park, « Thermogravimetric analysis of rice husk flour filled thermoplastic polymer composites », *Journal of thermal analysis and calorimetry*, vol.76, no2, p.395-404, 2004.
- [18] C. Zhao, H. Qin, F. Gong, M. Feng, S. Zhang, et M. Yang, « Mechanical, thermal and flammability properties of polyethylene/clay nanocomposites », *Polymer Degradation and Stability*, vol. 87, n° 1, p. 183-189, 2005.
- [19] K. Biswas, V. Khandelwal, et S. N. Maiti, « Rheological properties of teak wood flour reinforced HDPE and maize starch composites », *Journal of Applied Polymer Science*, vol. 138, n° 8, p. 49874, 2021, doi: 10.1002/app.49874.
- [20] K. J. Wilczynski, « Determination of viscosity curves of wood polymer composites based on limited rheological measurements », *Polimery*, vol. 63, n° 3, p. 213-218, 2018.
- [21] T. Yokohara, S. Nobukawa, et M. Yamaguchi, « Rheological properties of polymer composites with flexible fine fibers », *Journal of Rheology*, vol. 55, n° 6, p. 1205-1218, 2011.
- [22] N. Sombatsompop et R. Dangtangee, « Effects of the actual diameters and diameter ratios of barrels and dies on the elastic

- swell and entrance pressure drop of natural rubber in capillary die flow », *Journal of applied polymer science*, vol. 86, n° 7, p. 1762-1772, 2002.
- [23] H. Qin *et al.*, « Thermal stability and flammability of polypropylene/montmorillonite composites », *Polymer Degradation and Stability*, vol. 85, n° 2, p. 807-813, 2004.
- [24] N. E. Marcovich, M. M. Reboledo, J. Kenny, et M. I. Aranguren, « Rheology of particle suspensions in viscoelastic media. Wood flour-polypropylene melt », *Rheologica Acta*, vol. 43, n° 3, p. 293-303, 2004.
- [25] F. Michaud, « Rhéologie de panneaux composites bois/thermoplastiques sous chargement thermomécanique: aptitude au postformage », 2003.
- [26] V. Mazzanti et F. Mollica, « A Review of Wood Polymer Composites Rheology and Its Implications for Processing », *Polymers*, vol. 12, n° 10, Art. n° 10, oct. 2020, doi: 10.3390/polym12102304.
- [27] J. Tian, R. Zhang, Y. Wu, et P. Xue, « Additive manufacturing of wood flour/polyhydroxyalkanoates (PHA) fully bio-based composites based on micro-screw extrusion system », *Materials & Design*, vol. 199, p. 109418, 2021.
- [28] D. Ndiaye, A. M. Badji, et A. Tidjani, « Physical changes associated with gamma doses on wood/polypropylene composites », *Journal of composite materials*, vol. 48, no 25, p. 3063-3071, 2014.
- [29] X. Lv *et al.*, « Rheological Properties of Wood-Plastic Composites by 3D Numerical Simulations: Different Components », *Forests*, vol. 12, no 4, p. 417, 2021.
- [30] V. Hristov et S. Vasileva, « Dynamic mechanical and thermal properties of modified poly (propylene) wood fiber composites », *Macromolecular Materials and Engineering*, vol. 288, no 10, p. 798-806, 2003.
- [31] HUFENBACH, W., IBRAIM, F. Marques, LANGKAMP, A., *et al.* Charpy impact tests on composite structures – an experimental and numerical investigation. *Composites Science and Technology*, 2008, vol. 68, no 12, p. 2391-2400.
- [32] Eder, G.; Janeschitz Kriegl, H.; Liedauer, S.; *Prog. Polym. Sci.*, 15, 1990, p. 629.
- [33] Freyermouth F; Etude et modification des propriétés du poly (butylènesuccinate), un polyester biosourcé et biodégradable. Matériaux. INSA de Lyon, 2014.
- [34] P.V. Joseph, K. Joseph, S. Thomas, C.K.S. Pillai, V.S. Prasad, G. Groeninckx, Mariana Sarkissova, 2003; The thermal and crystallisation studies of short sisal fibre reinforced polypropylene composites; *Composites: Part A* 34, 253-266.
- [35] S.M. Luz, J. Del Tio, G.J.M. Rocha, A.R. Goncalves, A.P. Del'Arco Jr, 2008; Cellulose and cellulignin from sugarcane bagasse reinforced polypropylene composites: Effect of acetylation on mechanical and thermal properties, *Composites: Part A* 39, 1362-1369.
- [36] A. Kumar, S. Commereuc, et V. Verney, « Ageing of elastomers: A molecular approach based on rheological characterization », *POLYMER DEGRADATION AND STABILITY*, vol. 85, p. 751-757, août 2004, doi: 10.1016/j.polymdegradstab.2003.11.014.
- [37] K. Oßwald, K. Reincke, S. Döhler, U. Heuert, B. Langer, et W. Grellmann, « Aspects of the ageing of elastomeric materials », *International Polymer Science and Technology*, vol. 44, n° 12, p. 1-10, 2017.
- [38] Eskander, S. B., & Tawfik, M. E. (2019). Impacts of gamma irradiation on the properties of hardwood composite based on rice straw and recycled polystyrene foam wastes. *Polymer Composites*, 40(6), 2284-2291.
- [39] S. Gaudin, F. Fraisse, V. Verney, S. Commerceuc, R. Guyonnet, et A. Govin, « Etude rhéologique de nouveaux biocomposites bois - polymères biodégradables », p. 5.
- [40] J. Tian, R. Zhang, Y. Wu, et P. Xue, « Additive manufacturing of wood flour/polyhydroxyalkanoates (PHA) fully bio-based composites based on micro-screw extrusion system », *Materials & Design*, vol. 199, p. 109418, 2021.
- [41] Ndiaye, D., Badji, A. M., & Tidjani, A. (2014). Physical changes associated with gamma doses on wood / polypropylene composites. *Journal of composite materials*, 48(25), 3063-3071.
- [42] D. Ndiaye, « Contribution à l'étude de la caractérisation, des propriétés physico-mécaniques et du processus de photo vieillissement des composites bois polymères. », 2012.